HOKKAIDO UNIVERSITY

Title	Effect of the constituent networks of double-network gels on their mechanical properties and energy dissipation process
Author(s)	Nakajima, Tasuku; Kurokawa, Takayuki; Furukawa, Hidemitsu; Gong, Jian Ping
Citation	Soft Matter, 16(37), 8618-8627 https://doi.org/10.1039/D0SM01057J
Issue Date	2020-10-07
Doc URL	http://hdl.handle.net/2115/82904
Type	article (author version)
File Information	composition_submission_rev2_nohighlight.pdf

Instructions for use

ARTICLE

Effect of Constituent Networks of Double-Network Gels on their Mechanical Properties and Energy Dissipation Process

Tasuku Nakajima,*[a,b,c] Takayuki Kurokawa,[a,c] Hidemitsu Furukawa,[d] and Jian Ping Gong [a,b,c]

Double-network (DN) gels, consisting of brittle first and ductile second networks, possess extraordinary strength, extensibility, and fracture toughness while maintaining high solvent content. Herein, we prepared DN gels consisting of various concentrations of the first and second networks to investigate the effect of each network structure on the tensile and fracture properties of DN gels. The results showed that the tensile properties of DN gels before yielding are mainly dominated by the first network, serving as a skeleton, whereas the properties after necking are determined by both networks. Moreover, we found that the DN gels with significant energy dissipation capacities exhibit high fracture resistance. Thus, this study not only confirms the factors determining the mechanical characteristics of DN gels but also explains how the two networks concertedly improve the toughness of DN gels.

Introduction

Double-network (DN) gels are interpenetrating network gels with extremely high strength and toughness.[1–3] They are mechanically so robust that they can withstand a strike by a golf club.[4] Tough DN gels are comprised of two contrasting networks: the first weak and brittle network and the second stretchy and relatively strong network. This DN concept for toughening of soft materials is universal and principally applicable to rubbery polymeric materials comprising various chemical species, including synthetic and natural polymers.[3–11] The initial reports on DN gels confirmed the presence of a chemically (covalently) cross-linked polyelectrolyte network because their extreme swelling in water results in a brittle and weak network.[1] It was also reported that chemically cross-linked non-ionic polymer networks, whose network strands are sparse and close to their stretching limit, can also be used as a brittle and weak first network.[5–6] Moreover, physically (non-covalently) cross-linked brittle gels have been widely used as the first network for tough DN gels.[7–8]

DN gels possess superior mechanical properties to single-network gels. The elastic single-network gels made from flexible polymer strands typically show low tensile fracture stresses of approximately 0.1 MPa or less. The DN gels with the chemically cross-linked first network exhibit a high tensile fracture stress of 0.1–2 MPa while maintaining a significant tensile fracture

strain of 100–1,500%, which are strongly affected by the two network compositions.[12–14] The DN gels with the physically cross-linked first networks sometimes possess significantly enhanced properties such as Young's modulus of 30 MPa and fracture stress of 13 MPa shown by the DN gels with the triblock copolymer first network and fracture strain of 2,200% shown by the DN gels with the calcium alginate first network.[8,10] Fracture energy, which is an index of the resistance against crack propagation, of an elastic single network was determined to be 1–100 J m^{-2} following the well-accepted Lake-Thomas prediction for rubbery materials.[15,16] In contrast, the fracture energy of the DN gels with the chemical first network has been reported to be 100–4,000 J m^{-2} and that of the DN gels with the physical first network was found to be as high as 10,000 J m^{-2}. [8,14,16] Such high toughness of DN gels also contributes to their good fatigue resistance and the large adhesion energy of DN gel-solid interfaces.[17,18]

The excellent fracture resistance of DN gels is explained based on the internal fracture mechanism, that is, catastrophic fracture of the brittle first network prior to macroscopic failure of gels.[2] Because a tough DN gel is comprised of a brittle first network and a stretchy second network, under large deformation, strands or bonds in the brittle first network undergoes partial scission and fragmentation before the stretchy second network reaches the breaking point. In the case of the DN hydrogels with the chemical first network, the internal rupture of the first network strands was confirmed by the large and irreversible mechanical hysteresis,[12,19,20] decreasing modulus (Mullins effect) after deformation,[12,20] and the chemical detection of the covalent bond rupture of the network.[6,21,22] Regarding the internal fracture, some DN gels exhibit yielding upon uniaxial deformation.[12,19] In yielding of the DN gels, the first network loses its integrity due to fragmentation and the mechanical properties of the DN gels change from the first network-based stiffness to the second

a. Faculty of Advanced Life Science, Hokkaido University, N21W11, Kita-ku, Sapporo, Japan. Tel&Fax: +81-11-706-9016; E-mail: tasuku@sci.hokudai.ac.jp
b. WPI-ICReDD, Hokkaido University, N21W10, Kita-ku, Sapporo, Japan.
c. Soft Matter GI-CoRE. Hokkaido University, N21W11, Kita-ku, Sapporo, Japan.
d. Graduate School of Engineering, Yamagata University, Yonezawa, Japan.

network-based stretchability. Such a yielding phenomenon also occurs at the crack tip of the DN gels. When a DN gel with an initial crack is deformed, stress concentrates near the crack tip, leading to local deformation and yielding of the DN gels. Consequently, a wide yielding zone, called the damage zone, is formed around the crack tip of the DN gel prior to crack propagation.[23] Because the formation of the damage zone dissipates a significant amount of energy, the energy required to fracture the DN gel is significantly high. This explains the extraordinarily high fracture energies of the DN gels.[24,25]

Recently, this internal fracture of DN gels has been applied chemically to create muscle-like self-growing materials.[21] As the internal fracture of the chemical DN gels is covalent bond rupture, active chemical species such as radicals are formed at the end of the ruptured strands,[26] which can initiate chemical reactions inside the DN gels. Thus, when the DN gels containing monomers and cross-linkers are deformed, the generated radical induces radical polymerisation of the monomers and cross-linkers to synthesise a new polymer network inside the DN gels. As a result, the mechanical properties of the DN gels are significantly improved after such mechanical stimuli like muscle training. Since the radical generation in the deformed DN gels is originated from the internal fracture, concentration of the generated radical has been found to be almost proportional to irreversible hysteresis loss (energy dissipation density) of the DN gels.[21]

As mentioned earlier, DN gels show high mechanical robustness and unique internal fracture mechanisms in addition to the intrinsic properties of gels such as high water content. These properties make DN gels useful as tough medical and industrial materials, including tough and biocompatible artificial cartilage and soft conductive materials for electronics.[27,28] In addition, owing to their internal fracture-based self-growing ability, DN gels are considered self-adaptive materials capable of transforming their properties in response to their mechanical environment.[21,29] Each of these various possible applications requires tailor-made DN gels with adjustable mechanical and internal fracture properties for unique functions. In principle, the mechanical properties of DN gels can be controlled by tuning the composition of the two networks that comprise DN gels. Several researchers have synthesised a series of chemical DN gels with a variety of compositions to clarify the composition–mechanical properties relationship of the DN gels. For example, Na *et al.* varied the composition of the second network of to optimise the DN gels.[30] Matsuda *et al.* controlled the swelling ratio of the first network to obtain the yielding criterion of the DN gels.[31] These studies have partly clarified the relationships between the structural parameters and mechanical properties of DN gels. However, these studies only changed the composition of one network, not both networks. Because the mechanical behaviours of DN gels can be controlled by the synergistic effect of the first and second networks, comprehensive studies on the effects of the structures of the *two* networks on the mechanical properties of the DN gels are needed. Some of the authors have varied the two network compositions of the DN gels and measured their mechanical properties.[13] However, they only aimed to clarify the

toughening criterion of the DN gels. Therefore, the role of the compositions of the two networks must be studied further.

Herein, we intend to elucidate the effect of the two network compositions on the tensile properties, energy dissipation process, and fracture properties of the chemical DN gels. We use the typical chemically cross-linked DN gels, namely, poly(2-acrylamido-2-methylpropanesulfonic acid)/poly(acrylamide) double-network gels (PAMPS/PAAm DN gels), as a model system, which are original DN hydrogels and have been widely used in the previous studies.[1,2] We tuned mechanical properties of the DN gels by controlling the cross-linker concentration in feed for the first network preparation, c_{1st_MBAA}, and the monomer concentration in feed for the second network preparation, c_{AAm}. The structure and mechanical properties of each network are remarkably changed by c_{1st_MBAA} and c_{AAm}, and thus the properties of the DN gel can be effectively tuned by these factors. Tensile and tearing tests were performed on these gels to clarify how the compositions of the two networks determine the mechanical properties and energy dissipation process of the DN gels. Moreover, origins of the obtained composition-properties relationships are discussed by using the theoretical models.

Experiment

Materials.

We recrystallised 2-acrylamido-2-methylpropanesulfonic acid (AMPS, Toa Gosei Co., Ltd.) from methanol, acrylamide (AAm, Junsei Chemical Co., Ltd.) from chloroform and *N,N'*-methylenebis(acrylamide) (MBAA, Wako Pure Chemical Industries, Ltd.) from ethanol. 2-Oxoglutaric acid (Wako Pure Chemical Industries, Ltd.) was used as received.

t-DN gel preparation.

As has been clarified in previous studies, conventional DN gels prepared by two-step polymerisation contain internetwork bonds between the first and second networks. These bonds are formed due to copolymerisation of the second network with the unreacted cross-linker of the first network.[14,32] Truly independent DN gels, or simply *t*-DN gels, are a special type of DN gels that contains a negligible amount of covalent bonds between the two networks.[14] Because *t*-DN gels have simpler structures than the conventional DN gels, we prepared *t*-DN gels for the analysis of the properties of the DN gels. First, the first network precursor solutions were prepared from 1 M of AMPS, 1–16 mol% of MBAA as the cross-linker, and 0.1 mol% of 2-oxogultaric acid as the photo-initiator (the molar percentages are respect to the monomer). The solutions were then moved to an argon blanket and poured into glass moulds consisting of two soda-lime flat glass plates separated by silicone rubber as a spacer (the thicknesses of the glass plates and silicone rubber were 3 mm and 1 mm, respectively,). Photopolymerisation of PAMPS gels was performed by irradiation with 365 nm UV light (4 mW cm^{-2}) from both sides of the mould for 10 h. The PAMPS gels were then immersed in a 0.1 M 2-oxogultaric acid (photo-initiator) aqueous solution for 1 day. The samples were

irradiated with 365 nm UV light for 10 h to generate excess radicals in the gels. These radicals acted on the unreacted vinyl groups of the cross-linkers in the gels and rendered the vinyl groups inert. The PAMPS gels containing less unreacted vinyl groups in the cross-linker were immersed in pure water for 5 days to remove any excess photo-initiator. Pure water was replaced every day during immersion. These PAMPS gels were then immersed in the second network precursor aqueous solutions consisting of 1–8 M of AAm, 0.02 mol% of MBAA, and 0.01 mol% of 2-oxogultaric acid for at least 2 days. The solutions were replaced once during immersion. After immersion, the gels were sandwiched between two flat glass plates and wrapped with a plastic film in an argon blanket. Photo-polymerisation of the PAAm network was performed in the presence of PAMPS gels by irradiation with the 365 nm UV for 9 h. In this study, the term "t-DN(x-y)" is used to describe the compositions of the t-DN gels, where x is the cross-linker concentration of the first network precursor solutions in feed, c_{1st_MBAA} (mol%), and y is the monomer concentration of the second network precursor solutions in feed, c_{AAm} (M). The following mechanical tests were performed on these t-DN gels in the as-prepared state without immersion in any solvents.

Concentration of each component in the t-DN gels .

The volume swelling ratio of the PAMPS network in the t-DN gels, Q, is defined as V/V_0, where V and V_0 are the volumes of the as-prepared t-DN gel and the corresponding as-prepared PAMPS gel, respectively. V/V_0 is determined by $V/V_0 = (t/t_0)^3$, where t and t_0 are the thicknesses of the as-prepared t-DN gel and the corresponding as-prepared PAMPS gel, respectively, measured with a calliper. True monomer unit concentration of the first network in the t-DN gels, C_{1st}, is estimated as

$$C_{1st} = \frac{c_{AMPS}R}{Q} \tag{1}$$

where c_{AMPS} is the AMPS molar concentration in the first network precursor solutions in feed and R is the conversion ratio of the AMPS monomer to the PAMPS network. In this study, the former was 1 M and the latter was almost 100% after 8 h of polymerisation.

Uniaxial tensile test.

A commercial tensile-compressive tester (Tensilon RTC-1310A, Orientic, Co.) was used for the uniaxial tensile test. The test was performed on dumbbell-shaped specimens standardised to the JIS-K6251-7 size (gauge length: 12 mm; width: 2 mm; thickness: 1.6–3.0 mm) with a fixed tensile velocity at 100 mm/min., corresponding to an initial strain rate of 0.14 s^{-1}. Nominal strain, ε, was calculated by dividing displacement of the tester by the initial gauge length. Note that the strain thus determined might be overestimated for large deformation. An extensometer was not used for determining the strain because some DN gels exhibit too large extensibility that is beyond the measurement limit. Young's modulus E was determined as the slope of the nominal stress–strain curves at $0 < \varepsilon < 0.1$. The fracture strain, ε_f, was determined as the nominal strain at the fracture point.

The yield stress, σ_y, was determined as the nominal stress at the zero-slope point of the stress–strain curves. All the values shown are averages of at least three measurements.

Tearing test.

The tearing energy, T, was determined through a tearing test on trouser-shaped specimens standardised to the JIS-K6252 1/2 size (50 mm in length (with 20 mm long initial legs) and 7.5 mm in width) using a Tensilon RTC-1310A. The tearing test was performed in mode III loading mode by pulling one leg of the specimen at a velocity of 500 mm/min while the other leg was fixed. Thus, the tearing velocity at a crack tip is about 250 mm/min at the steady state crack growth. The energy required to fracture a unit area of a sample was estimated as $T = 2F_{ave}/t$ without consideration of stretch of the legs, where F_{ave} is the average tearing resistance force and t is the thickness of the gel.[23] Since the leg stretch is neglected, the obtained tearing energy by the above equation is underestimated a little but not far from the actual value considering the leg stretch. In fact, tearing energy of the typical DN gel with and without considering leg stretch have been reported as 991 and 935 J m^{-2}, respectively.[33] All the values shown are averages of at least three measurements.

Mechanical hysteresis measurement.

Cycle tensile tests were performed with a commercial tensile tester Instron 5965 (Instron Co.) and a noncontact video extensometer (AVE, Instron Co.). The gels were cut into dumbbell-shaped pieces and standardised to the JIS-K6251-7 size. The samples were first uniaxially stretched to the desired strain, ε_{max}, and then immediately unloaded (the unloading process was not recorded) with a fixed tensile velocity at 100 mm/min. After reaching their original length, the samples were immediately elongated beyond ε_{max}. In general, mechanical hysteresis measurements were performed by measuring the cycle of the loading and unloading curves. For DN gels, it is known that the second loading curve completely overlaps with the first unloading curve. Thus, we measured the second loading curves instead of the unloading curves in this study. The dissipated energy density, $U_{hys}(\varepsilon_{max})$ (J m^{-3}), which is defined as the area between the first and second loading curves at the maximum strain ε_{max} of the first loading, was calculated as

$$U_{hys}(\varepsilon_{max}) = \int_0^{\varepsilon_{max}} (\sigma_1 - \sigma_2)\, d\varepsilon \tag{2}$$

where σ_1 and σ_2 are the nominal stresses of the first and second loading curves, respectively. Note that these notations are not the same as σ_{1st} and σ_{2nd}, which are defined later as the stresses of the first and second networks, respectively.

Results and discussion

Swelling of the first network.

We synthesised 35 types of t-DN gels with different compositions of the two networks by varying the cross-linker concentration of the first network precursor solutions, c_{1st_MBAA}

(mol%), and the monomer concentration of the second network precursor solutions, c_{AAm} (M). These t-DN gels are called as t-DN(x-y) gels, where x is c_{1st_MBAA} and y is c_{AAm}. They showed a wide variety of mechanical properties, all of which were transparent and uniform to the eye, regardless of the change in composition. First, we characterised swelling properties of the first network in the t-DN gels. The first PAMPS network largely swelled in the second network precursor aqueous solution due to polyelectrolyte nature of PAMPS. Note that swelling ratio of the PAMPS gels in the second precursor solutions is independent of their AAm concentration c_{AAm}. Large swelling of a polyelectrolyte gel in polar solvent is due to contribution of movable dissociated counterions to total osmotic pressure of a gel. According to the Manning's condensation theory, ratio of the movable counterions among total ones of a polyelectrolyte chain is dominated by dielectric constant of the solution.[34] Thus, independency of Q of the PAMPS gels from the AAm concentration means that effect of AAm concentration on dielectric constant of the second precursor solution is negligible.

Figure 1(a) depicts the volume swelling ratio, Q, of the PAMPS network in the as-prepared t-DN gels synthesised using various cross-linker concentrations, c_{1st_MBAA}. As cross-linking suppresses the swelling of networks, a higher cross-linker concentration in the PAMPS network leads to less swelling of the network in the AAm aqueous solution, and therefore to a small Q. Figure 1(b) depicts the dependence of the first network concentration of the t-DN gel, C_{1st}, on c_{1st_MBAA}, indicating that an increase in the cross-linker concentration leads to an increase in the C_{1st}. Here, we obtained power-law relationships between Q or C_{1st} and c_{1st_MBAA} as

$$Q \propto c_{1st\_MBAA}^{-1.14} \tag{3a}$$

$$C_{1st} \propto c_{1st\_MBAA}^{1.14} \tag{3b}$$

Ideally, segment number of a network strand of the first network N is inversely proportional to the ratio of cross-linker concentration c_{1st_MBAA} to monomer concentration c_{AMPS} used for the first network synthesis;

$$N \propto \frac{c_{AMPS}}{c_{1st\_MBAA}} \tag{4}$$

Considering constant c_{AMPS}, we rewrite eqn (3) by using N as;

$$Q \propto N^{1.14} \tag{5a}$$

$$C_{1st} \propto N^{-1.14} \tag{5a}$$

This relationship is consistent to the theoretical prediction. To derive this relationship theoretically, we adopt the tension blob (Pincus blob) model to the network strands of the swollen first network.[35,36] According to this model, the network strand with N segments under tension is represented by a series of tension blobs with g segments lined up along the tension direction. Number of tension blobs per a strand is thus N/g. Segments in each tension blob are unperturbed, thus average size and thermal energy of each tension blob are $\xi = bg^{\nu}$ and of the order of kT, respectively, where b is segment length and ν is Flory exponent. Considering the balance of osmotic pressure

due to movable (uncondensed) counterions and elastic pressure of an equilibrium swollen polyelectrolyte gel, one can obtain $g = \alpha^{-1}$ for a polyelectrolyte gel, where α is a ratio of movable counterions among total counterions in the gel and should be constant in this case.[37] Considering the average end-to-end distance of a network strand at as-prepared state is bN^{ν}, one can describe equilibrium swelling ratio of the first network gel in a salt-free medium as;

$$Q = \left(\frac{\xi N g^{-1}}{bN^{\nu}}\right)^3 = \left(\frac{bN\alpha^{1-\nu}}{bN^{\nu}}\right)^3 = (\alpha N)^{3(1-\nu)} \propto N^{3(1-\nu)} \tag{6a}$$

By using $Q \propto C_{1st}^{-1}$,

$$C_{1st} \propto N^{3(\nu-1)} \tag{6b}$$

can be also derived. Substitution of ν=0.6 for a real chain to eqn (6) leads $Q \propto N^{1.2}$ and $C_{1st} \propto N^{-1.2}$, which are enough close to the experimental eqn (5). Slight deviation of the experimental results from the theory implies that the ideal eqn (6a) does not perfectly explain the results. Possible reasons of the deviation include the effect of osmotic pressure due to the mixing of the polymer and the solvent and the electrostatic repulsion between the charges fixed on polymers, which were ignored during the derivation of eqn (6) for simplicity.
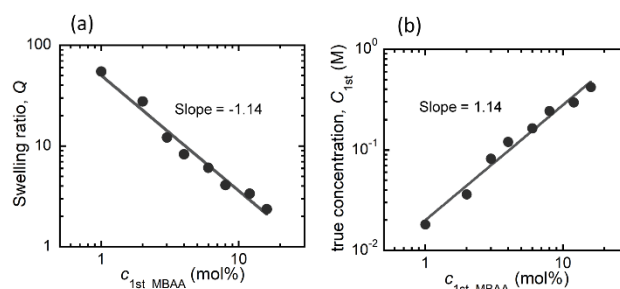

Figure 1. Effect of cross-linker concentration of the first network precursor solution, c_{1st_MBAA} (mol%), on (a) the swelling ratio Q and (b) true first network concentration, C_{1st} (M), of the as-prepared t-DN gels. Q was independent of the AAm concentration c_{AAm} and the error bars are hidden by the symbols.
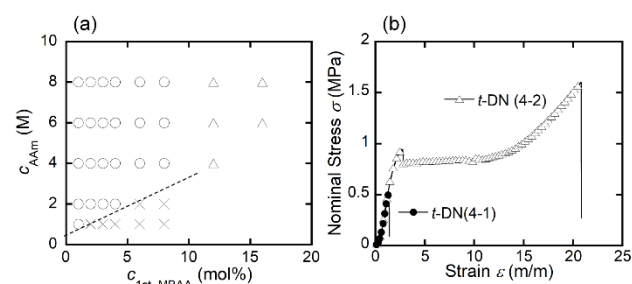

Figure 2. (a) The tensile behaviour diagram of the t-DN(x-y) gels with various x-y combinations. Circle symbols denote the stretchy DN gels, cross symbol denotes the brittle DN gels and triangle symbols denote the DN gels broken just after yield point. All the experimental data were observed on as-prepared DN gels. (b) Typical examples of stress-strain curves of the stretchy DN gel (t-DN(4-2) gel) and the brittle DN gel (t-DN(4-1) gel).

Tensile behaviour of *t*-DN gels.

The synthesised *t*-DN gels can be classified into brittle and stretchy groups based on their tensile mechanical behaviours. Figure 2(a) depicts the tensile behaviour diagram of the *t*-DN(*x*-*y*) gels in the *x*-*y* space, and typical tensile stress–strain curves for the brittle and stretchy groups are shown in Figure 2(b). The stretchy DN gels (circle in Figure 2(a)) were mechanically robust and showed yielding and significantly high fracture strain, which are the features of tough DN gels.[2] In contrast, the brittle DN gels (cross) could be easily broken. They do not have any characteristics of tough DN gels, such as yielding, high fracture stress, and high fracture strain. As exceptions, some DN gels with high c_{1st_MBAA} break just after reaching the yield point; thus, they are classified into the intermediate group (triangle). As quantitatively discussed in a previous experimental and theoretical papers, altering the balance of the strengths of the two networks leads to this transition.[13,38] In order for DN gels to be tough, the relative strength of the second network to the first network must be enough large. When the AAm concentration, c_{AAm}, was below a critical value, the DN gels showed a brittle behaviour due to insufficient strength of the second network. In contrast, when the AAm concentration was higher than the critical value, the DN gels became stretchy. This critical concentration of c_{AAm} depended on c_{1st_MBAA} as strength of the first network increases with c_{1st_MBAA}.

From this section, we focus on the mechanical properties of the stretchy *t*-DN gels marked as circles in Figure 2(b). Figure 3 depicts the tensile stress–strain curves for the *t*-DN(*x*-4) and *t*-DN(4-*y*) gels, where *x* and *y* were 2–8 (mol%) and 2–8 (M), respectively. The different contributions of each network to the stress–strain curves of the DN gels were determined. As depicted in Figure 3(a), *x* (c_{1st_MBAA}) strongly affects the stress–strain curves of the DN gels. With an increase in c_{1st_MBAA}, the tensile stress of the DN gels significantly increases from the origin to the fracture point. In contrast, the effect of the second network is found mainly after reaching the yield point (Figure 3(b)). Before reaching the yield point, even though c_{AAm} was varied from 2 to 8 M, the tensile curves of the DN(4-*y*) gels were nearly coincident. In contrast, after reaching the yield point, the higher the second network concentration, the higher the tensile stress. Next, we discuss the reason for the different contributions of the two networks. The yield point of DN gels has been considered as the point where the brittle first network reaches its stretching limit.[31] Thus, before the yield point, the first network is in a highly stretched state and shows obvious strain hardening, whereas the second network remains in a coiled state. Thus, the mechanical properties of DN gels in this regime are dominated by the stiff first network. The dominance of the first network on the mechanical properties of pre-necked DN gels has already been pointed out by Ducrot *et al.* and by some of authors.[31,39] In contrast, after reaching the yield point, the first network is considered to be ruptured into discontinuous pieces, which are topologically connected by the second network through entanglement.[40] In such cases, the second network contribution to the mechanical behaviour of DN gels can no longer be ignored, whereas the remaining first network serving as macroscopic cross-linking points continues to contribute to the mechanical behaviour. Thus, after reaching the yield point, the mechanical properties of the DN gels are determined by both networks.
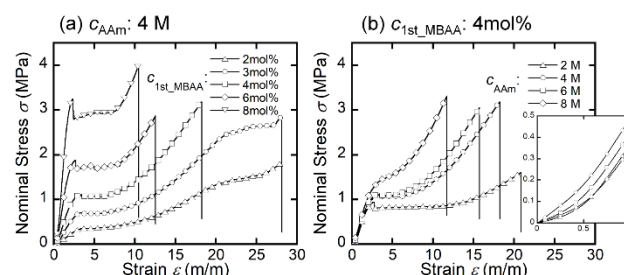

Figure 3. The tensile stress-strain curves of (a) the *t*-DN(*x*-4) gels and (b) the *t*-DN(4-*y*) gels where $x=c_{1st\_MBAA}$ and $y=c_{2nd}$ are 2–8 (mol%) and 2–8 (M), respectively. The tensile velocity was fixed at 100 mm/min. The insert figure in (b) shows the enlarged small strain region.
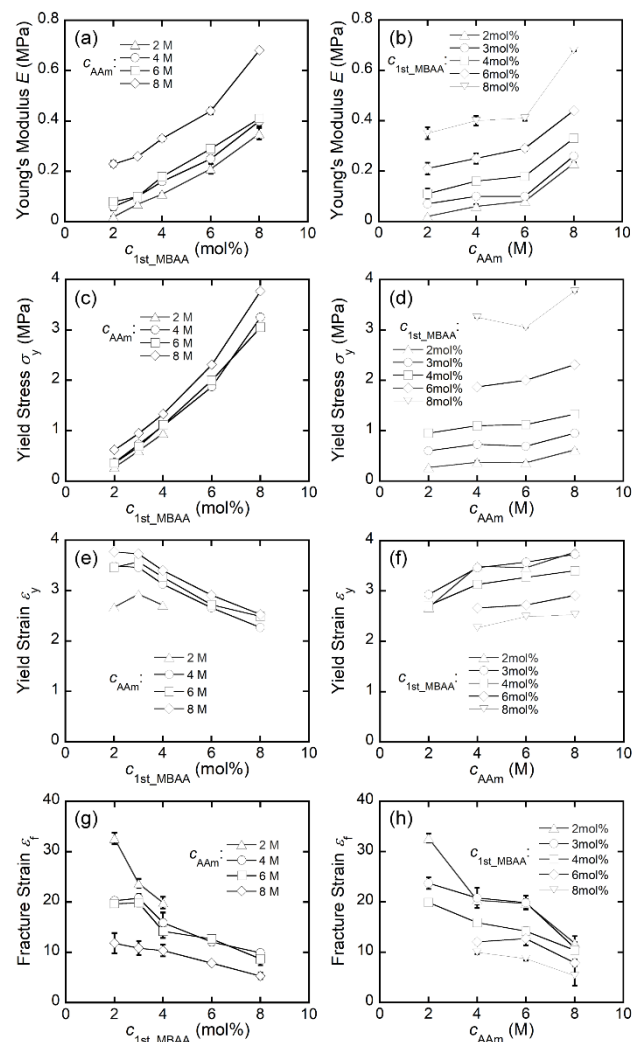

Figure 4. Composition dependencies of (a-b) the Young's modulus, *E*, (c-d) the yield stress, σ_y, (e-f) the yield strain, ε_y, and (g-h) the fracture strain, ε_f, of the *t*-DN gels measured by the tensile test.

Figure 4 exhibits the dependence of various mechanical properties on the t-DN gel compositions. Figure 4(a,b) shows the elastic modulus, E, and Figure 4(c,d) shows the yield stress, σ_y, of the t-DN gels with different compositions. The E and σ_y of the t-DN gels significantly increase with c_{1st_MBAA}, but are less dependent on c_{AAm}. The optimised DN gel with the dense first network (t-DN(8-8)) showed the elastic modulus of 0.7 MPa and the yield stress of 3.7 MPa. Furthermore, among the non-stretchy DN gels, t-DN(16-8) showed the highest elastic modulus of 1.3 MPa and the highest yield stress of 8.4 MPa. Figure 4(e,f) shows the yield strain of the t-DN gels. The yield strain is weakly dependent on both c_{1st_MBAA} and c_{AAm}. Figure 4(g,h) shows the fracture strain, ε_f, of the t-DN gels of various compositions. Note that the values of ε_f should contains some systematic errors such as overestimation due to not using extensometer and possible effect of sample geometry on fracture points of the DN gels. Nevertheless, these figures show the trend between ε_f and compositions. One can see that ε_f tends to decrease with an increase in both c_{1st_MBAA} and c_{AAm}, and the t-DN gels with low c_{1st_MBAA} and c_{AAm} show high extensibility.

Herein, the dependences of the above mechanical properties of the t-DN gels on both c_{1st_MBAA} and c_{AAm} are analysed. For the elastic modulus, let DN gels be assumed to be a simple bi-continuous composite material, wherein their elasticity is simply the sum of the two components. Under this assumption, the E of the DN gels at small strain can be assumed to be

$$E \approx E_{1st} + E_{2nd} \qquad (7)$$

where E_{1st} and E_{2nd} are the elastic moduli of the first and second networks, respectively. For the as-prepared DN gels, E_{1st}, which is elastic modulus of the polyelectrolyte first network gel at swelling equilibrium in a salt-free medium, should be nearly proportional to its true polymer concentration C_{1st},[36] thus;

$$E_{1st} \approx E - E_{2nd} \propto C_{1st} \qquad (8)$$

We plot E of the t-DN gels against C_{1st} as shown in Figure 5(a). For the t-DN gels with the same c_{AAm}, the obtained $E - C_{1st}$ curves are almost linear regardless to c_{AAm}, and the slope of the linear regression curves are almost constant, suggesting validity of the eqn (8). On the other hand, the curves are slightly convex downward especially for c_{AAm}=8 M, implying contribution of inter-network entanglements to Young's modulus of the DN gels.[13,40] The larger first and second network concentrations give the denser internetwork entanglements, which may lead nonlinear increase of the modulus at larger C_{1st}. Importance of the inter-network entanglement will be also mentioned in the discussion of the fracture strain.

According to our previous study, yield point of DN gels is where the first network reaches its maximum allowable strain ($\approx$yield strain), ε_y, thus ε_y has been known to be almost independent of the second network composition.[31] Under the assumption of affine deformation in which macroscopic deformation corresponds to microscopic deformation, the yield point of DN gel is considered to be the point at which the first network strands reach their contour length. Thus, the following equation can be derived;

$$\frac{bN}{bN^\nu} = N^{1-\nu} \approx Q^{\frac{1}{3}}(\varepsilon_y + 1) \qquad (9)$$

This equation expresses that the network strand of the first network reaches its contour length bN by the swelling $Q^{1/3}$ times from the as-prepared state and the stretching ε_y+1 times. Here, by using eqn (6a), one can derive $Q^{1/3} \propto N^{1-\nu}$. Combination of this relationship and eqn (9) leads the prediction that the yield strain does not depend on the first network composition. Since ε_y+1 of DN gels is almost equal to the average end-to-end distance of the first network strands with respect to their contour length, this theoretical prediction (independency of ε_y) means that the size of the first network strands relative to their contour length should be constant regardless of c_{1st_MBAA}. In the actual experiments, slight negative correlation between ε_y and c_{1st_MBAA} was observed, probably because of the non-ideal swelling of the first network discussed in the analysis of swelling behaviour.

For the nominal yield stress σ_y, the previous study shows that the yield stress of DN gels is proportional to their area densityof the first network strands at the unstretched state, d, as $\sigma_y \propto d$. The area density is given by;

$$d \approx \nu_e^{\frac{2}{3}} \propto \left(\frac{C_{1st}}{N}\right)^{\frac{2}{3}} \qquad (10)$$

where ν_e is density of the elastically effective first network strands. Substitution of eqn (6b) to eqn (10) leads

$$\sigma_y \propto d \propto c_{1st}^{\frac{2(3\nu-4)}{9(\nu-1)}} \qquad (11)$$

Substitution of ν =0.6 to eqn (11) leads the theoretical relationship $\sigma_y \propto C_{1st}^{1.22}$. To confirm this prediction, the experimental dependence of σ_y on C_{1st} was plotted (Figure 5(b)). We observed a power-law relationship $\sigma_y \propto C_{1st}^{1.13}$, which is enough close to the theoretical estimation.

The dependence of ε_f on c_{1st_MBAA} and c_{AAm} can be understood as follows. After the first network ruptures into discontinuous fragments, the mechanical properties of the DN gels changed to the second network-based stretchy ones.[12] Thus, the extensibility of DN gels after yielding should be mainly determined by the second network cross-linking density. Since the second network is sufficiently dense and interpenetrates with the first network, three types of cross-linking of the second
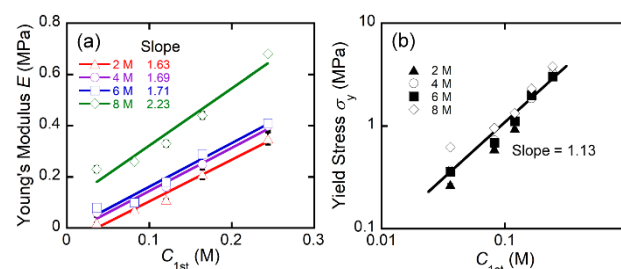

Figure 5. The relationships between (a) E and C_{1st} and (b) σ_y and C_{1st} of the t-DN gels.
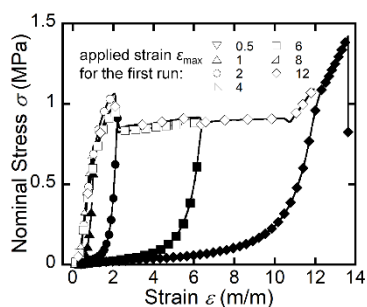
Figure 6. Successive loading curves (hysteresis loops) of the t-DN(4-2) gels measured by the tensile hysteresis measurement. The numbers for each symbol denote the applied strain, ε_{max} of the first loading curve. The open symbols denote the first loading curves (undamaged samples) and the filled symbols denote the second loading curves (damaged samples). $U_{hys}(\varepsilon_{max})$ is defined as the area between the first and second loading curves.
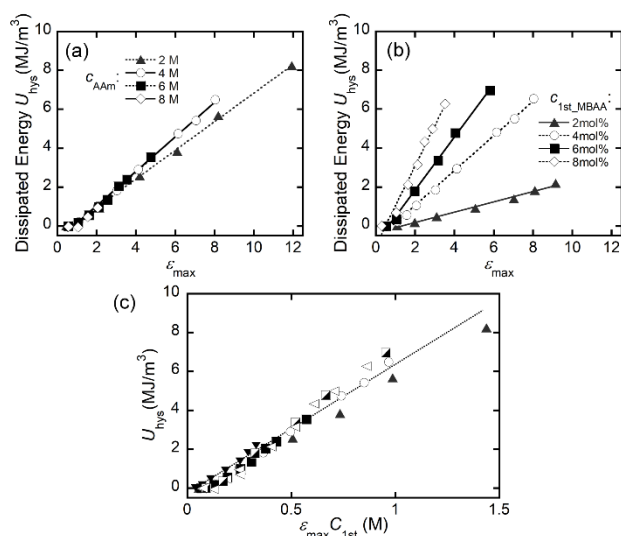

Figure 7. (a) The dissipated energy, U_{hys}, of the t-DN(4-y) gels as a function of the applied strain, ε_{max}. (b) U_{hys} of the t-DN(x-4) gels as a function of ε_{max}. (c) The dependence of the U_{hys} on $\varepsilon_{max}C_{1st}$ of the t-DN gels. The symbols in Figure 7(c) correspond to the symbols used in Figures 7(a) and (b). The dashed line is provided as a guide to the eye.

network are possible: covalent cross-linking, intra-network entanglement,[41] and inter-network entanglement between the second and first networks.[30,40] Covalent cross-linking is formed by co-polymerisation of the divinyl cross-linker MBAA with the monomer AAm. Because the feed ratio of MBAA to AAm was fixed at 1/5000 regardless of c_{AAm}, if the chemical cross-linking determines the fracture strain, it should depend on neither c_{AAm} nor c_{1st_MBAA}. In addition, if the intra-network entanglement in the second network determines the fracture strain, it should only depend on c_{AAm}. However, the actual ε_f strongly depends on both c_{AAm} and c_{1st_MBAA}, suggesting the inter-network entanglement between the first and second networks should dominate the fracture strain ε_f. As the entanglement density increases with the concentration of both components, ε_f of the DN gels qualitatively decreases when both c_{AAm} and c_{1st_MBAA} increase.

Mechanical hysteresis loss.

The mechanical hysteresis in the cycle tensile tests was characterised to clarify the energy dissipation process of the

various t-DN gels upon uniaxial deformation. Note that strain is correctly measured in this experiment by using an extensometer. Figure 6 depicts the cyclic tensile test results of the t-DN(4-2) gels, which show extremely large and irreversible mechanical hysteresis in agreement with other DN gels reported in previous studies.[12,16,19] The area between the first and the second loading curves at the desired strain ε_{max}, defined as the dissipated energy density, $U_{hys}(\varepsilon_{max})$, is a parameter used to characterise the amount of energy consumed during the tensile deformation due to internal fracture of the first network. U_{hys} increases with an increase in ε_{max}, even in the hardening region, which is in agreement with our previous report.[12] Figure 7(a) depicts the dependence of U_{hys} on ε_{max} of the DN gels consisting of the same first network but different second network concentrations, t-DN(4-y) gels (y = 2–8 M). The graphs almost overlap regardless of the second

network concentration, with a linear relationship between U_{hys} and ε_{max}. Figure 7(b) depicts the dependence of U_{hys} on ε_{max} for the DN gels consisting of the same second network but different first network, t-DN(x-4) gels (x = 2–8 mol%). The results strongly depend on c_{1st_MBAA}. All samples show a linear relationship between U_{hys} and ε_{max}, similar to the t-DN(4-y) gels, whereas the slope significantly increases with an increase in c_{1st_MBAA}. As the high c_{1st_MBAA} leads to a high first network concentration c_{1st}, the result in Figure 7(b) indicates that the energy required for fracturing the first network increases with an increase in its concentration c_{1st}. As the linear relation between U_{hys} and ε_{max} roughly goes through the coordinate origin, we obtain $dU_{hys}/d\varepsilon_{max} \approx U_{hys}(\varepsilon_{max})/\varepsilon_{max}$. In Figure 7(c), we plotted U_{hys} against $\varepsilon_{max}C_{1st}$ and found the empirical relationship;

$$U_{hys} \propto \varepsilon_{max}C_{1st} \tag{12}$$

Eqn (12) is the general relationship applicable for both t-DN(4-y) and (x-4) gels. This equation does not include a term related to the second network, suggesting that the energy dissipation (internal fracture process of the first network) of the DN gels upon stretching is independent of the second network. In other words, the existence of the second network does not affect the internal fracture of the first network in the DN gels. This discussion may seem to be in conflict with the previous discussion about fracture strain, which concludes that the fracture strain of DN gels is determined partly by the entanglement between the first and second networks. This conflict may be due to the different nature of the two networks. The strands of the brittle first network are almost fully stretched, whereas the strands of the stretchy second network are soft and flexible. Thus, the existence of inter-network entanglement may not affect the deformation and fracture behaviours of the first network but may strongly affect the behaviour of the soft second network.

The structural origin of eqn (12) can be discussed as follows. According to the discussion in ref. 12 based on the Lake-Thomas theory, total energy required for the internal fracture of the first network in DN gels is given by
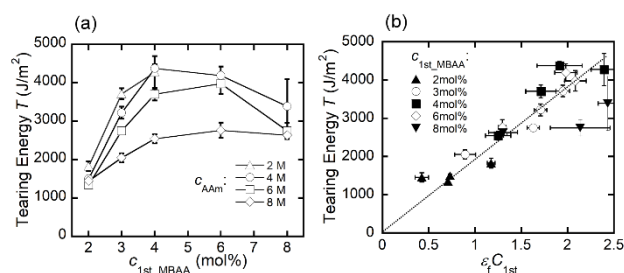
Figure 8. (a) Composition dependencies of the tearing energy, T, of the t-DN gels. The t-DN(6-2) and t-DN(8-2) gels were too brittle to be measured by the tearing test. The tearing velocity was fixed at 250 mm/min. (b) The dependence of the T on $\varepsilon_f C_{1st}$ of the t-DN gels. The dashed line is provided as a guide to the eye.

$$U_{hys}(\varepsilon_{max}) \propto C_{1st}\varphi_b(\varepsilon_{max}) \tag{13}$$

where φ_b is the fracture ratio of the first network strand at a certain strain.[12] On the other hand, as already shown in the discussion on the yield strain, it is expected for the as-prepared t-DN gels that the average end-to-end distance of the first network strands with respect to their contour length should be constant regardless of c_{1st_MBAA}. Similarly, it is expected that the end-to-end distance distribution of the strands with respect to the contour length also does not depend on c_{1st_MBAA}. Under this assumption, φ_b at a certain strain is expected to be independent of c_{1st_MBAA}. Eqn (12) is derived by substitution of this relationship to eqn (13) at ε_{max}.

The dissipated energy density at the fracture point, $U_{hys,f}$, is the maximum energy dissipation capacity of the DN gels and could be an important material parameter. From eqn (5), $U_{hys,f}$ can be estimated as

$$U_{hys,f} \propto \varepsilon_f C_{1st} \tag{14}$$

Because the fracture strain, ε_f, is related to the compositions of both networks, eqn (14) indicates that $U_{hys,f}$ is affected by both networks. To be precise, the energy dissipation rate, $dU_{hys}/d\varepsilon_{max}$, is determined only by the first network structure, whereas the maximum extensibility, ε_f, is determined by both networks.

Fracture behaviour.

We performed the trouser tear test to the t-DN gels to determine their tearing energy, T. Figure 8(a) depicts the T of the stretchy t-DN gels at various concentrations. T of the t-DN gel showed a maximum value at a certain optimum c_{1st_MBAA}, irrespective of its second network concentration. The optimised compositions for the largest T of approximately 4,000 J/m² are c_{1st_MBAA} = 4–6 mol% and c_{AAm} = 2–4 M. The similar tendency has already been reported in physically crosslinked DN gels.[8]

For the fracture energy of DN gels, Brown and Tanaka independently proposed fracture models that explain the high toughness of DN gels.[24] Their common assumption for the high fracture energy of a DN gel is the formation of a strip-like damage zone around a fracture surface. Prior to the crack propagation of DN gels, the local region ahead of a crack tip is stretched to become a softer "damage zone", accompanied by significant energy dissipation due to the internal fracture in this region. Crack propagation is initiated when the characteristic

thickness of the damage zone reaches a certain value, h. Thus, the T of the DN gels is the sum of the intrinsic T of the damage zone, T_0, and the dissipated energy due to the formation of the damage zone, T_{dis}, as

$$T = T_0 + T_{dis} \cong T_0 + U_{dis}h \tag{15}$$

where U_{dis} is the characteristic energy dissipation density in the damage zone. The formation of the damage zone and the occurrence of the internal fracture of the DN materials in the damage zone have been experimentally confirmed, which supports the validity of their models.[21] By considering $T \gg T_0$, eqn (15) can be simplified as

$$T \cong U_{dis}h \tag{16}$$

Here, it can be assumed that the DN gels showing a high maximum energy dissipation capacity, $U_{hys,f}$, also show a high characteristic energy dissipation density, U_{dis}, upon fracturing. This idea and eqn (12) give

$$U_{dis} \propto U_{hys,f} \propto \varepsilon_f C_{1st} \tag{17}$$

Based on eqn (16) and (17), we compared the T of the DN gels with the $\varepsilon_f C_{1st}$, as shown in Figure 8(b). A proportional relationship between T and $\varepsilon_f C_{1st}$ was found experimentally. This relationship provides the empirical design principle for the synthesis of tough DN gels with high fracture resistance, that is, the high maximum energy dissipation capacity, $U_{hys,f} = \varepsilon_f C_{1st}$, leading to the high tearing energy T of the DN gels;

$$T \propto U_{hys,f} \propto \varepsilon_f C_{1st} \tag{18}$$

This relationship corresponds to the basic idea of Brown and Tanaka. Since origin of high toughness of DN gels is the energy dissipation due to the internal fracture of the first network near the crack tip, it is acceptable that the larger the maximum energy dissipation capacity of DN gels leads their larger tearing energy. The similar data have been found for several DN gels with the physical first network.[8,42] Moreover, same tendency has been also found for tough soft materials (without double-network structure) toughened by the energy dissipation mechanism,[43] suggesting the concept of eqn (18) is applicable not only to DN gel but also to various tough soft materials.

Although we have obtained the empirical guiding principle to obtain the high toughness of the DN gels, the underlying relationship between the energy dissipation capacity and the real damage zone structure around a crack tip of the DN gels is still not clear at this time. In this work we have not mentioned the damage zone thickness, h, of the t-DN gels although not only U_{dis} but also h must affect the fracture energy of the DN gels according to eqn (15). To this end, we note that while the model by Brown and Tanaka simply assumes a homogeneous damage zone, the real damage zone should have a damage gradient from a crack surface to the edge. Thus, future investigations on the damage gradient are necessary to completely understand the relationship between toughness and composition of the DN gels. Such damage gradient has been observed in the multiple network elastomers having similar toughening mechanism.[44] As a separately study, we are also investigating the damage

distribution near the fracture surface of DN gels. The results of that investigation will be published in future papers.

Conclusions

First, we highlighted the contributions of the two networks to the tensile stress–strain curves of the DN gels. Initial mechanical response and yield stress of the DN gels are mainly dominated by the stiff and brittle first network but weakly depend on the stretchy second network. After reaching the yield point where the first network breaks into fragments, mechanical response and fracture strain of the DN gels are determined by both network structures, where the second component serves as network strands and the fragmented first network may work as macroscopic cross-linking points through the inter-network entanglements. These knowledges contribute to synthesis of DN gels showing desired mechanical responses at various strains. Second, the internal fracture process of various t-DN gels was analysed. We found that the internal fracture rate, $dU_{hys}/d\varepsilon_{max}$, is determined only by the first network but not by the second network. On the other hand, the maximum energy dissipation capacity of the DN gels, $U_{hys,f}$, was dominated by both the networks because it depends on not only the internal fracture rate but also the fracture strain. Since a larger $U_{hys,f}$ corresponds to a larger mechanoradical generation capacity upon deformation, this finding is useful for synthesizing self-growing DN gels that exhibit efficient mechanoradical polymerization against mechanical stimuli.[19] Third, we found the empirical criterion for preparation of DN gels with high fracture energy. This result supports the existing fracture model of the DN gels and contributes to creation of tougher DN gels. These behaviours provide a deeper insight into how the specific topological structure of the DN gels contribute to the mechanical response and toughness of DN gels.

Conflicts of interest

There are no conflicts of interest to declare.

Acknowledgements

Notes and references

1   J. P. Gong, Y. Katsuyama, T. Kurokawa and Y. Osada, *Adv. Mater.*, 2003, **15**, 1155–1158.
2   J. P. Gong, *Soft Matter*, 2010, **6**, 2583–2590.
3   T. Nakajima, *Polym. J.*, 2017, **49**, 477–485.
4   T. Nakajima, N. Takedomi, T. Kurokawa, H. Furukawa and J. P. Gong, *Polym. Chem.*, 2010, **1**, 693.
5   T. Nakajima, H. Sato, Y. Zhao, S. Kawahara, T. Kurokawa, K. Sugahara and J. P. Gong, *Adv. Funct. Mater.*, 2012, **22**, 4426–4432; T. Nakajima, Y. Ozaki, R. Namba, K. Ota, Y. Maida, T. Matsuda, T. Kurokawa and J. P. Gong, *ACS Macro Lett.*, 2019, **8**, 1407–1412.
6   E. Ducrot, Y. Chen, M. Bulters, R. P. Sijbesma and C. Creton, *Science*, 2014, **344**, 186–189.
7   W. Yang, H. Furukawa and J. P. Gong, *Adv. Mater.*, 2008, **20**, 4499–4503; Q. Chen, L. Zhu, C. Zhao, Q. Wang and J. Zheng, *Adv. Mater.*, 2013, **25**, 4171–4176.
8   J.-Y. Sun, X. Zhao, W. R. K. Illeperuma, O. Chaudhuri, K. H. Oh, D. J. Mooney, J. J. Vlassak and Z. Suo, *Nature*, 2012, **489**, 133–136.
9   X. Feng, Z. Ma, J. V. MacArthur, C. J. Giuffre, A. F. Bastawros and W. Hong, *Soft Matter*, 2016, **12**, 8999–9006.
10 H. J. Zhang, T. L. Sun, A. K. Zhang, Y. Ikura, T. Nakajima, T. Nonoyama, T. Kurokawa, O. Ito, H. Ishitobi and J. P. Gong, *Adv. Mater.*, 2016, **28**, 4884–4890; H. J. Zhang, F. Luo, Y. Ye, T. L. Sun, T. Nonoyama, T. Kurokawa and T. Nakajima, *ACS Appl. Polym. Mater.*, 2019, **1**, 1948–1953.
11 L. Yuan, Y. Wu, Q. sheng Gu, H. El-Hamshary, M. El-Newehy and X. Mo, *Int. J. Biol. Macromol.*, 2017, **96**, 569–577; Y. Wang, Z. Wang, K. Wu, J. Wu, G. Meng, Z. Liu and X. Guo, *Carbohydr. Polym.*, 2017, **168**, 112–120.
12 T. Nakajima, T. Kurokawa, S. Ahmed, W. L. Wu and J. P. Gong, *Soft Matter*, 2013, **9**, 1955–1966.
13 S. Ahmed, T. Nakajima, T. Kurokawa, M. Anamul Haque and J. P. Gong, *Polymer*, 2014, **55**, 914–923.
14 T. Nakajima, H. Furukawa, Y. Tanaka, T. Kurokawa, Y. Osada and J. P. Gong, *Macromolecules*, 2009, **42**, 2184–2189.
15 G. J. Lake and A. G. Thomas, *Proc. R. Soc. A Math. Phys. Eng. Sci.*, 1967, **300**, 108–119.; Y. Akagi, H. Sakurai, J. P. Gong, U. Il Chung and T. Sakai, *J. Chem. Phys.*, 2013, **139**, 13251–13258.
16 Y. Tanaka, R. Kuwabara, Y. H. Na, T. Kurokawa, J. P. Gong and Y. Osada, *J. Phys. Chem. B*, 2005, **109**, 11559–11562.
17 R. Bai, Q. Yang, J. Tang, X. P. Morelle and J. Vlassak, *Extrem. Mech. Lett.*, 2017, **15**, 91–96.; W. Zhang, X. Liu, J. Wang, J. Tang, J. Hu, T. Lu and Z. Suo, *Eng. Fract. Mech.*, 2018, **187**, 74–93.
18 J. Li, A. D. Celiz, J. Yang, Q. Yang, I. Wamala, W. Whyte, B. R. Seo, N. V. Vasilyev, J. J. Vlassak, Z. Suo and D. J. Mooney, *Science*, 2017, **357**, 378–381.; R. Takahashi, K. Shimano, H. Okazaki, T. Kurokawa, T. Nakajima, T. Nonoyama, D. R. King and J. P. Gong, *Adv. Mater. Interfaces*, 2018, **5**, 1–10.
19 Y.-H. Na, Y. Tanaka, Y. Kawauchi, H. Furukawa, T. Sumiyoshi, J. P. Gong and Y. Osada, *Macromolecules*, 2006, **39**, 4641–4645.
20 R. E. Webber, C. Creton, H. R. Brown and J. P. Gong, *Macromolecules*, 2007, **40**, 2919–2927.
21 T. Matsuda, R. Kawakami, R. Namba, T. Nakajima and J. P. Gong, *Science*, 2019, **363**, 504–508.
22 P. Millereau, E. Ducrot, J. M. Clough, M. E. Wiseman, H. R. Brown, R. P. Sijbesma and C. Creton, *Proc. Natl. Acad. Sci. U. S. A.*, 2018, **115**, 9110–9115.
23 Y. Tanaka, Y. Kawauchi, T. Kurokawa, H. Furukawa, T. Okajima and J. P. Gong, *Macromol. Rapid Commun.*, 2008, **29**, 1514–1520; Q. M. Yu, Y. Tanaka, H. Furukawa, T. Kurokawa and J. P. Gong, *Macromolecules*, 2009, **42**, 3852–3855.
24 H. R. Brown, *Macromolecules*, 2007, **40**, 3815–3818; Y. Tanaka, *Europhys. Lett.*, 2007, **78**, 56005.
25 R. Long and C.-Y. Hui, *Soft Matter*, 2016, **12**, 8069–8086.
26 J. Sohma, *Prog. Polym. Sci.*, 1989, **14**, 451–596.
27 K. Arakaki, N. Kitamura, H. Fujiki, T. Kurokawa, M. Iwamoto, M. Ueno, F. Kanaya, Y. Osada, J. P. Gong and K. Yasuda, *J. Biomed. Mater. Res. - Part A*, 2010, **93**, 1160–1168.
28 S. Naficy, J. M. Razal, G. M. Spinks, G. G. Wallace and P. G. Whitten, *Chem. Mater.*, 2012, **24**, 3425–3433.
29 S. Craig, *Science*, 2019, **363**, 451–452.
30 Y.-H. Na, T. Kurokawa, Y. Katsuyama, H. Tsukeshiba, J. P. Gong, Y. Osada, S. Okabe, T. Karino and M. Shibayama, *Macromolecules*, 2004, **37**, 5370–5374.

31 T. Matsuda, T. Nakajima, Y. Fukuda, W. Hong, T. Sakai, T. Kurokawa, U. Il Chung and J. P. Gong, *Macromolecules*, 2016, **49**, 1865–1872.

32 S. S. Es-Haghi, A. I. Leonov and R. A. Weiss, *Macromolecules*, 2013, **46**, 6203–6208.

33 T. Matsuda, T. Nakajima, R. Kawakami and J. P. Gong, 2020, chemrxiv.12555419.v1.

34 G. S. Manning, J. Chem. Phys., 1969, 51, 924–933.

35 P. Pincus, Macromolecules, 1976, 9, 386–388; J.-L. Barrat, J.-F. Joanny and P. Pincus, *J. Phys. II*, 1992, **2**, 1531–1544.

36 M. Rubinstein, R. H. Colby, A. V. Dobrynin and J.-F. Joanny, *Macromolecules*, 1996, **29**, 398–406.

37 B. A. Mann, C. Holm and K. Kremer, J. Chem. Phys., 2005, **122**, 154903.

38 X. Wang and W. Hong, *Soft Matter*, 2011, **7**, 8576–8581; X. Zhao, *J. Mech. Phys. Solids*, 2012, **60**, 319–332.

39 E. Ducrot and C. Creton, *Adv. Funct. Mater.*, 2016, **26**, 2482–2492.

40 M. Huang, H. Furukawa, Y. Tanaka, T. Nakajima, Y. Osada and J. P. Gong, *Macromolecules*, 2007, **40**, 6658–6664.

41 M. Rubinstein and R. H. Colby, *Polymer Physics*, Oxford University Press, New York, 2003.

42 Q. Chen, D. Wei, H. Chen, L. Zhu, C. Jiao, G. Liu, L. Huang, J. Yang, L. Wang and J. Zheng, *Macromolecules*, 2015, **48**, 8003–8010.

43 A. Klein, P. G. Whitten, K. Resch and G. Pinter, *J. Polym. Sci. Part B Polym. Phys.*, 2015, **53**, 1763–1773.; K. Mayumi, J. Guo. T. Narita, C. Y. Hui and C. Creton, Ext. Mech. Lett. 2016, **6**, 52–59.

44 Y. Chen, C. J. Yeh, Y. Qi, R. Long and C. Creton, *Sci. Adv.*, 2020, **6**, eaaz5093.